Active rotational and translational microrheology beyond the linear spring regime

Lachlan J. Gibson, Shu Zhang, Alexander B. Stilgoe, Timo A. Nieminen, and Halina Rubinsztein-Dunlop
The University of Queensland, School of Mathematics and Physics, Brisbane QLD 4072, Australia
(Received 9 March 2017; revised manuscript received 5 April 2017; published 24 April 2017)

Active particle tracking microrheometers have the potential to perform accurate broadband measurements of viscoelasticity within microscopic systems. Generally, their largest possible precision is limited by Brownian motion and low frequency changes to the system. The signal to noise ratio is usually improved by increasing the size of the driven motion compared to the Brownian as well as averaging over repeated measurements. New theory is presented here whereby error in measurements of the complex shear modulus can be significantly reduced by analyzing the motion of a spherical particle driven by nonlinear forces. In some scenarios error can be further reduced by applying a variable transformation which linearizes the equation of motion. This enables normalization that eliminates error introduced by low frequency drift in the particle's equilibrium position. Our measurements indicate that this can further resolve an additional decade of viscoelasticity at high frequencies. Using this method will easily increase the signal strength enough to significantly reduce the measurement time for the same error. Thus the method is more conducive to measuring viscoelasticity in slowly changing microscopic systems, such as a living cell.

DOI: 10.1103/PhysRevE.95.042608

I. INTRODUCTION

The strength of a microrheometer can be assessed by its ability to perform accurate broadband measurements of viscoelasticity within microscopic systems. In particular, there is great interest in improving methods for conducting measurements within living biological systems, such as a cell [1–5].

Particle tracking microrheometers have proven to be a good candidate for accomplishing such a task [4–6]. They work by tracking the motion of one or more particles embedded in the pertinent medium. The complex shear modulus $G^*(\omega)$, a frequency (ω) dependent measure of linear viscoelasticity, can be inferred from the way the particles move [7–9].

Biological systems are often very small or highly inhomogeneous [10]. So, tracking only a single particle can be more practical since the measurement is more localized than a multiparticle system. The motion of a single tracked particle can either be driven passively, where Brownian motion is the primary driving force, or actively, where Brownian motion acts as a noise on top of another external driving force. For example, Bennett *et al.* [8] trapped a single spherical birefringent particle using optical tweezers. The particle's birefringence also allowed it to be angularly trapped when using a linearly polarized laser beam. In this particular example, the angular motion driven by thermal fluctuations allowed $G^*(\omega)$ to be calculated using statistical methods including autocorrelations. Therefore, passive methods tend to be more successful at measuring higher frequency viscoelasticity. Conversely, passive methods require too much time to resolve lower frequency viscoelasticity precisely [9,11] in slowly changing systems [12,13].

Active methods, in which the particle is driven by some other force, often eliminate Brownian noise by averaging over a repeated motion. The average Brownian motion decreases towards zero, leaving only the nonstochastic motion. For example, Preece *et al.* [9] used optical tweezers to trap a spherical particle within two alternating spatially offset traps. The particle switched between one stable equilibrium to another when one beam was turned off and the other turned on. The linear motion of the particle as it fell into each trap was measured and used to calculate $G^*(\omega)$.

Evidently, it is possible to measure viscoelasticity by examining either rotational or linear motion. Therefore, the aim of this paper is to outline and test a generalized theory applicable to either kind of motion. This theory describes how to obtain $G^*(\omega)$ from repeated measurements of a particle falling into an equilibrium position under the influence of both Brownian noise and a position dependent force.

For the sake of simplicity, the previous theory (such as that used by Preece *et al.*) assumed a force that is linearly dependent on position. For small displacements this is often a valid assumption. However, as will be subsequently shown in Sec. III, the signal strength can be significantly increased by allowing the particle to fall into position from outside the linear regime. Increasing the signal strength of each individual measurement can appreciably reduce the total measurement time, thereby justifying application of this method in dynamic biological systems such as a living cell. Therefore, the theory outlined here accounts for nonlinear driving forces (not to be confused with nonlinear motion or nonlinear viscoelasticity).

To confirm the validity of the theory in at least one example, experimental measurements in both viscous and viscoelastic fluids conducted by an optical tweezers microrheometer are also examined. The different analysis methods for the same data are applied to compare the accuracy as well as the frequency range in which the viscoelasticity can be resolved.

It should be stressed that although the theory is only experimentally verified in this paper using optical tweezers measurements, the analysis is not predicated on that mode of particle manipulation. Provided the driving force is characterizable, this theory could also be applied to many other systems such as magnetic or acoustic tweezers.

II. THEORY

For simplicity, the following theory is expressed in terms of rotational dynamics. However, obtaining the corresponding results for linear motion at any step can be achieved by a simple substitution. Angle, moment of inertia, torque, and rotational drag can be replaced by their respective linear counterparts: linear position, mass, force, and linear drag.

A. Equation of motion

1. jth flip Langevin equation

Consider a microscopic spherical particle centered at the origin with a fixed center of mass. The particle, embedded in a fluid with linear viscoelasticity, is free to rotate about the z axis guided by Brownian motion, viscoelastic drag, and an angular dependent driving torque. The particle should have a stable equilibrium angle such that it becomes trapped at a root of the driving torque function. Repeatedly dropping the particle into the trap from an outside position allows the Brownian noise to be mitigated by averaging many drops.

With a moment of inertia I the stochastic evolution of the azimuthal angle (ϕ_j) of the jth drop can be modeled by a generalized Langevin equation [7,8]

$$I\ddot{\phi}_j = \tau_j(t) - \int_{-\infty}^{t} \zeta(t - t_l)\dot{\phi}_j(t_l)\, dt_l - \chi T(\phi_j). \qquad (1)$$

The total toque ($I\ddot{\phi}_j$) on the sphere at time t is the sum of the driving torque $[-\chi T(\phi_j)]$ that forms the trap, the viscoelastic torque $[-\int_{-\infty}^{t} \zeta(t - t_l)\dot{\phi}_j(t_l)dt_l$ with generalized memory function $\zeta(t)]$ from the fluid, and the thermal toque $[\tau_j(t)]$ from Brownian motion.

2. Driving torque function properties

Without loss of generality, the stable equilibrium angle is set to 0 with positive trap stiffness χ so that $T(0) = 0$ and $T'(0) = 1$. In contrast to the dot symbol in Eq. (1) which denoted a time derivative, here the prime symbol indicates a spatial derivative. The trap potential is assumed to be symmetric about the equilibrium whereby the so called driving torque function, $T(\phi)$, is a continuously differentiable odd function. Hence, for small deviations about the equilibrium, the Taylor series of $T(\phi)$ to fifth order is given by

$$T(\phi) = \phi + \frac{T_3}{3!}\phi^3 + \frac{T_5}{5!}\phi^5 + \cdots , \qquad (2)$$

where $T_n = T^{(n)}(0)$. Notice that all even terms in the series are zero since $T(\phi)$ is an odd function.

In order for the particle to be pulled into the $\phi = 0$ equilibrium, the driving torque must have opposite sign to the position. Therefore, the torque function must have the same sign as the position, $\mathrm{sign}(T(\phi)) = \mathrm{sign}(\phi)$. This requirement can limit the allowed positions if the torque changes sign. Therefore, if there exists an angle $\phi = R > 0$ such that $T(R) = 0$ then the domain must be restricted to $|\phi| < R$. Similarly, if there exists a singularity at angle $\phi = R > 0$ such that $\lim_{\phi\to R} T(\phi)^{-1} = 0$, then the domain is also restricted to $|\phi| < R$. Since this restriction applies to all roots and singularities (except for $\phi = 0$) R is chosen to be the smallest positive root or singularity. If $T(\phi)$ has no additional roots to $\phi = 0$ and is continuously differentiable over all $\mathbb{R}$, then the domain is unrestricted, $\phi \in \mathbb{R}$.

3. Stokes flow

Particle tracking microrheometers typically operate with microscopic particles. Therefore, it is likely that the fluid has a low Reynolds number ($\mathscr{R} \ll 1$) and hence undergoes Stokes flow [8]. The inertial term $I\ddot{\phi}_j$ in Eq. (1) is, consequently, negligible relative to the others and can be ignored:

$$\tau_j(t) = \int_{-\infty}^{t} \zeta(t - t_l)\dot{\phi}_j(t_l)\, dt_l + \chi T(\phi_j). \qquad (3)$$

4. Generalized memory function

The time dependent generalized memory function, $\zeta(t)$, describes the ratio of viscoelastic torque to an instantaneous step rotation of the particle. Hence, it is proportional to the fluid's relaxation modulus [7],

$$\zeta(t) = \alpha G_r(t), \qquad (4)$$

where α depends on the geometry of the probe particle as well as the type of motion. Therefore, the Langevin equation relates the fluid viscoelastiticy to the angular position by

$$\tau(t) = \alpha \int_{-\infty}^{t} G_r(t - t_l)\dot{\phi}_j(t_l)\, dt_l + \chi T(\phi_j). \qquad (5)$$

For a sphere of radius a undergoing rotational or linear motion,

$$\alpha = 8\pi a^3 \quad \text{or} \quad \alpha = 6\pi a \qquad (6)$$

respectively [14].

B. Linear case

1. Normalization

If $T(\phi)$ is a nonlinear function, then the Langevin equation (5) is a nonlinear differential equation. This poses a problem for any repeated measurements in which the initial position of each flip varies. If the Langevin equation were linear then the position could be normalized by dividing the equation by the initial angle.

Previously, to obtain a linear differential equation the flipping angle was assumed to be small such that the driving torque could be approximated by its Taylor series [Eq. (2)] to first order,

$$T(\phi) \approx \phi. \qquad (7)$$

In this case, transforming to the normalized angle $\varphi_j = \frac{\phi_j}{\phi_j(0)}$ so that $\varphi_j(0) = 1$ gives

$$\frac{\tau_j(t)}{\phi_j(0)} = \alpha \int_{-\infty}^{t} G_r(t - t_l)\dot{\varphi}_j(t_l)\, dt_l + \chi\varphi_j. \qquad (8)$$

Notice that after normalization the Brownian motion term is inversely proportional to the initial position $\phi_j(0)$. Therefore, to minimize the effect of Brownian motion the initial angle should be maximized, but only within the allowed domain that satisfies the Taylor series small angle approximation. Thus, there exists some optimal angle whereby the total error contributed by Brownian motion and the Taylor series is minimized. The value of this optimal angle and relative error is quantified later in Sec. III A.

2. Average flip

The Brownian noise can be reduced by averaging n repeated flips. Assuming each flip is independent of the others, the normalized linear Langevin equations (8) for each rotation can be averaged,

$$0 = \alpha \int_0^t G_r(t - t_l)\dot{\varphi}(t_l)\, dt_l + \chi\varphi. \tag{9}$$

φ represents the expected normalized angle and is estimated using a finite average of all n flips,

$$\varphi \approx \frac{1}{n}\sum_{j=1}^{n} \varphi_j. \tag{10}$$

Provided that the time between flips is much longer than the time it takes for the particle to reach equilibrium, each flip should "forget" the previous one and finish with an average velocity of zero. Mathematically, this is expressed as $\dot{\varphi}(t) = 0$, for $t < 0$, which truncates the memory integral at $t = 0$. The average Brownian motion is also assumed to be zero, removing the corresponding term entirely.

3. Viscous fluid

A purely viscous fluid without any elasticity does not "remember" any past motion. Its relaxation modulus is proportional to a Dirac delta function, $G_r(t) = \eta\delta(t)$, where η is the dynamic viscosity. With this relaxation modulus, Eq. (9) simplifies to a simple first order ordinary differential equation,

$$0 = \alpha\eta\dot{\varphi} + \chi\varphi, \tag{11}$$

with a well known solution,

$$\varphi = e^{-kt}, \quad \text{where } k = \frac{\chi}{\alpha\eta}. \tag{12}$$

Evidently, the viscosity is inversely related to the decay rate of the angle over time, k.

4. Unilateral Fourier transform

More generally, obtaining linear viscoelasticity from the dynamics requires the use of a unilateral Fourier transform (UFT). Represented by a tilde, the UFT is defined by

$$\tilde{f}(\omega) = \int_0^\infty f(t)e^{-i\omega t}\, dt. \tag{13}$$

Applying the UFT to Eq. (9) transforms the convolution integral into a product that can be easily manipulated,

$$0 = \alpha\tilde{G}_r(\omega)(i\omega\tilde{\varphi} - 1) + \chi\tilde{\varphi}. \tag{14}$$

The relaxation modulus, $G_r(t)$, is related to the time domain conjugate of $G^*(\omega)$ by

$$G^*(\omega) = i\omega\tilde{G}_r(\omega). \tag{15}$$

Therefore, $G^*(\omega)$ can be expressed in terms of $\tilde{\varphi}$ by rearranging Eq. (14),

$$G^*(\omega) = \frac{\chi}{\alpha}\frac{i\omega\tilde{\varphi}}{1 - i\omega\tilde{\varphi}}. \tag{16}$$

Equation 16 relates the linear viscoelasticity to the average motion of the particle at different time scales.

C. Nonlinear case

The theory presented thus far acts mostly as a summary of already known methodology for the purpose of juxtaposition. This section will now adjust the theory to account for a nonlinear driving torque function.

1. Viscous case

Consider the average behavior given by a nonlinear driving torque function in a viscous fluid. The Langevin equation is similar to Eq. (11), but is a nonlinear ordinary differential equation,

$$0 = \alpha\eta\dot{\phi} + \chi T(\phi). \tag{17}$$

Notice the assumption that

$$T(\phi) \approx \frac{1}{n}\sum_{j=1}^{n} T(\phi_j), \tag{18}$$

which should be valid provided the deviations from the average of each individual flip are not too large.

2. Variable transform

The nonlinearity of Eq. (17) makes it nonnormalizable in terms of ϕ. However, applying a variable transformation can make it normalizable in terms of a different variable,

$$\Psi(\phi) = \exp\left(\int \frac{d\phi}{T(\phi)}\right). \tag{19}$$

More specifically, the new position variable Ψ is defined as the solution to

$$\Psi = T\Psi', \quad \text{such that } \Psi'(0) = 1. \tag{20}$$

Applying this transformation linearizes Eq. (17),

$$0 = \alpha\eta\dot{\Psi} + \chi\Psi, \tag{21}$$

which, like the viscous linear case, has an exponential solution,

$$\psi = e^{-kt}, \quad \text{where } \psi = \frac{\Psi}{\Psi(\phi_0)} \text{ and } \phi_0 = \phi(0). \tag{22}$$

3. Properties of Ψ

The definition of Ψ in Eq. (20) ensures that it is a strictly increasing continuously differentiable odd function of ϕ over the whole domain.

Its Taylor series is given by

$$\Psi(\phi) = \phi + \frac{-T_3}{2\times 3!}\phi^3 + \frac{5T_3^2 - T_5}{4\times 5!}\phi^5 + \cdots, \tag{23}$$

where the derivatives of Ψ at $\phi = 0$ can be expressed in a recursive form as a discrete convolution,

$$\Psi_n = -n!\sum_{j=1}^{\frac{n-1}{2}} \frac{n-2j}{n-1}\frac{\Psi_{n-2j}}{(n-2j)!}\frac{T_{2j+1}}{(2j+1)!}, \tag{24}$$

where $\Psi_n = \Psi^{(n)}(0)$ and $\Psi_1 = 1$.

Finding the radius of convergence of this Taylor series in general has proved difficult. However, by dividing Eq. (24) by Ψ_n and taking the $n \to \infty$ limit, it can be shown that if $\Psi_i \geqslant 0$ for all derivatives, then the radius of convergence either covers the whole domain or is at least as large as the radius of convergence of the $T(\phi)$ Taylor series described in Sec. II A 2.

4. Solution in terms of ϕ by inverting Ψ

Finding the solution to Eq. (17) in terms of the original position variable, ϕ, can be achieved by applying the inverse variable transformation to the solution in terms of Ψ given by Eq. (22),

$$\phi = \Psi^{-1}(\Psi) = \Psi^{-1}(\Psi(\phi_0)e^{-kt}). \tag{25}$$

The Taylor series of the inverse function $\Psi^{-1}(\Psi)$ can be found by series reversion [15] of Eq. (23),

$$\Psi^{-1}(\Psi) = \Psi + \frac{T_3}{2\times 3!}\Psi^3 + \frac{5T_3^2+T_5}{4\times 5!}\Psi^5 + \cdots. \tag{26}$$

Therefore, by applying the Taylor series of both Ψ and Ψ^{-1} to Eq. (25), the solution to Eq. (17) in terms of time and initial position can be found in a series form,

$$\phi = \phi_0 e^{-kt} - \phi_0^3(e^{-kt} - e^{-3kt})\frac{T_3}{2\times 3!} + \cdots. \tag{27}$$

Notice that the series is always exactly correct at the time bounds $t = 0$ and $t \to \infty$ irrespective of the degree at which it may be truncated. The first term is the solution under the small angle approximation, and each successive term adds corrections to the position between the time bounds.

5. Unnormalized analysis viscoelastic fluid

Now consider the average dynamics of a particle in a viscoelastic fluid driven by a nonlinear torque function. Without normalization, Eq. (5) can be averaged. Similar to Eq. (9), the average thermal torque and angular velocity for $t < 0$ are zero,

$$0 = \alpha\int_0^t G_r(t-t_l)\dot{\phi}(t_l)\,dt_l + \chi T(\phi). \tag{28}$$

Following the steps outlined in Sec. II B 4, applying the unilateral Fourier transform allows $G^*(\omega)$ to be evaluated,

$$G^*(\omega) = \frac{\chi}{\alpha}\frac{i\omega\tilde{T}}{\phi_0 - i\omega\tilde{\phi}}. \tag{29}$$

Notice that the transform of the torque function is evaluated using its implicit time dependence via $T(\phi(t))$. This expression has a similar form to Eq. (16); however, the nonlinearity of $\tilde{T}$ means that it must depend on the initial position ϕ_0. Therefore, any variation in the initial position due to slow changes in the system or apparatus can introduce error to the calculated result.

6. Viscoelastic fluid with variable transformation

Motivated by the successful linearization in the viscous case, the same variable transform is applied to Eq. (3), which models the dynamics of the jth flip driven by a nonlinear driving torque function in a viscoelastic fluid,

$$\frac{\tau_j(t)}{f(t)} = \alpha\int_{-\infty}^t G_r(t-t_l)\dot{\psi}_j(t_l)\frac{f(t_l)}{f(t)}\,dt_l + \chi\psi_j, \tag{30}$$

$$\text{where } f(t) = \frac{T(\phi(t))}{\psi(t)} = \frac{\Psi(\phi_0)}{\Psi'(\phi)}. \tag{31}$$

Now it is assumed that the fluid memory function decays much faster than the time of the flip, so that

$$\frac{f(t_l)}{f(t)} \approx 1. \tag{32}$$

Notice that, this condition is exactly met in a viscous fluid which has no "memory." Conversely, for an elastic solid the memory function never decays to zero, so this assumption would invariably fail. Making the approximation simplifies the Langevin equation to a normalizable form reminiscent of the linear case,

$$\frac{\tau_j(t)}{f(t)} = \alpha\int_{-\infty}^t G_r(t-t_l)\dot{\psi}_j(t_l)\,dt_l + \chi\psi_j. \tag{33}$$

Following the same steps of averaging and transforming outlined in Sec. II B allows the complex shear modulus to be calculated,

$$G^*(\omega) = \frac{\chi}{\alpha}\frac{i\omega\tilde{\psi}}{1 - i\omega\tilde{\psi}}. \tag{34}$$

Evidently, this expression of $G^*(\omega)$ is very similar to Eq. (16) where the new normalized position variable ψ has taken over the role of φ. Notice that in this case minimizing the Brownian motion term involves maximizing $f(t)$. Generally this also involves increasing ϕ_0; however, the allowed domain is much larger without the Taylor series small angle approximation. Instead the maximum value is only limited by the slow flip time (relative to the fluid memory function) assumption.

III. ERROR ANALYSIS

This section aims to quantify the theoretical relative error of both both the old and new methods of analysis. This can help compare both methods and also determine the optimal initial position which minimizes these errors.

A. Linear case

1. Error in complex shear modulus

As outlined in Sec. II B, maximizing the signal to noise ratio involves increasing the initial position. However, since the driving torque function is only approximately linear for small angles, increasing ϕ_0 too much will introduce systematic errors larger than the random error caused by Brownian motion. To quantify these errors $G^*(\omega)$ is calculated directly from the multiple flip average of Eq. (5), except this time the linear torque and zero mean thermal torque approximations are not imposed, $T(\phi) \neq \phi$ and $\tau \neq 0$, where τ is the average thermal torque:

$$G^*(\omega) = \frac{\chi}{\alpha}\frac{i\omega}{\phi_0 - i\omega\tilde{\phi}}\left(\tilde{\phi} + (\tilde{T} - \tilde{\phi}) - \frac{\tilde{\tau}}{\chi}\right). \tag{35}$$

Therefore, the absolute relative error in $G^*(\omega)$ can be evaluated by

$$\delta G^*_{\text{Lin}} = \left|\frac{\tilde{T} - \tilde{\phi}}{\tilde{\phi}} - \frac{\tilde{\tau}}{\chi\tilde{\phi}}\right|. \tag{36}$$

2. Average thermal torque

The average thermal torque defined by

$$\tau(t) = \frac{1}{n}\sum_{j=1}^{n}\tau_j(t) \tag{37}$$

only approaches zero as $n \to \infty$. For a finite number of flips the average Brownian motion will still have a thermal torque with standard deviation decaying with $n^{-1/2}$.

Therefore, assuming the thermal torque is white noise, the unilateral Fourier transform of τ should have a constant magnitude that also decays with $n^{-1/2}$. The phase of $\tilde{\tau}$ at each frequency should be random meaning that the expected real and imaginary parts are both zero. Therefore, in calculating the following expected errors, terms proportional to $\tilde{\tau}$ or the real or imaginary parts of $\tilde{\tau}$ can be ignored. So, the expected relative error in the linear case should be

$$\delta G^*_{\mathrm{Lin}} = \sqrt{\left|\frac{\tilde{T} - \tilde{\phi}}{\tilde{\phi}}\right|^2 + \left|\frac{\tilde{\tau}}{\chi\tilde{\phi}}\right|^2}. \tag{38}$$

3. High frequency error

An expression for the relative error at high frequencies can be found by employing the initial value theorem, whereby the unilateral Fourier transform at high frequencies can be asymptotically related to the initial value of the function in the time domain,

$$\tilde{f}(\omega) \sim \frac{f(0)}{i\omega}. \tag{39}$$

Applying the initial value theorem as well as the Taylor series of $T(\phi)$ to third order yields

$$\delta G^*_{\mathrm{Lin}} = \left|\frac{T_3}{6}\phi_0^2 - \frac{i\omega\tilde{\tau}}{\chi\phi_0}\right| = \sqrt{\left(\frac{T_3}{6}\phi_0^2\right)^2 + \left(\frac{\omega|\tilde{\tau}|}{\chi\phi_0}\right)^2}. \tag{40}$$

Fixing the frequency to ω_0 allows the optimal initial angle for a particular frequency to be found via standard calculus optimization,

$$\phi_0 = \left(\frac{3\sqrt{2}\omega_0|\tilde{\tau}|}{|T_3|\chi.}\right)^{\frac{1}{3}} \tag{41}$$

This particular value of ϕ_0 gives a total relative error of

$$\delta G^*_{\mathrm{Lin}} = \sqrt{2\omega^2 + \omega_0^2}\left(\frac{|T_3||\tilde{\tau}|^2}{12\chi^2\omega_0}\right)^{\frac{1}{3}}. \tag{42}$$

Notice that this error is proportional to $|\tilde{\tau}|^{2/3}$, meaning that the error decays with the number of flips by $n^{-1/3}$. This means, at least for high frequencies, halving the relative error requires eight times the number of flips.

B. Nonlinear case

1. Error in complex shear modulus

Next we consider the relative error of $G^*(\omega)$ when accounting for a nonlinear driving torque, as given by the analysis outlined in Sec. II C 5. The error contribution from Brownian motion can be established by including the thermal noise term in Eq. (28). This yields an expression for $G^*(\omega)$,

$$G^*(\omega) = \frac{\chi}{\alpha}\frac{i\omega}{\phi_0 - i\omega\tilde{\phi}}\left(\tilde{T} - \frac{\tilde{\tau}}{\chi}\right), \tag{43}$$

with an absolute relative error of

$$\delta G^*_{NLin} = \left|\frac{\tilde{\tau}}{\chi\tilde{T}}\right|. \tag{44}$$

Unlike the linear case, Brownian motion is the primary source of error, so here the relative error is proportional to $|\tilde{\tau}|$. Hence, the relative error reduces with the number of flips at a faster rate of $n^{-1/2}$.

2. High frequency error

Applying the initial value theorem shows that at high frequencies the minimum error is obtained by maximizing the initial driving torque,

$$\delta G^*_{NLin} = \frac{\omega|\tilde{\tau}|}{\chi T(\phi_0)}. \tag{45}$$

3. Low frequency error in a viscous fluid

From Eq. (17), in a viscous fluid $\tilde{T} = \frac{\phi_0}{k}$ for $\omega = 0$. Therefore, the error is given by

$$\delta G^*_{NLin} = \frac{k|\tilde{\tau}|}{\chi\phi_0}, \tag{46}$$

which is minimized by maximizing the initial position. These results suggest that an initial position larger than the position which maximizes the driving torque should be chosen to reduce error.

IV. EXPERIMENTAL RESULTS

Measurements of $G^*(\omega)$ were conducted in both viscous and viscoelastic fluids to compare the accuracy and precision of the new analysis methods. Applying the same methodology outlined by Zhang *et al.* [16], optical tweezers were employed to rotationally trap a spherical vaterite probe particle. The particle rotates between two stable equilibrium angles by alternating between two angularly offset linearly polarized beams.

In this case, the restoring torque function is sinusoidal $T(\phi) = 1/2\sin(2\phi)$ because of the wave-plate nature of the vaterite probe particles [17]. Therefore, the variable transformation is $\Psi = \tan\phi$ and the optimal initial angle should be within $\pi/4 \leqslant \phi_0 < \pi/2$. For measurements presented here $\phi_0 \approx 70^\circ$, well beyond the linear regime.

Measurements were conducted in water, a viscous fluid, as well as dilutions (50% and 100% by weight) of Celluvisc (Allergan) eyedrops, a strongly viscoelastic fluid. $G^*(\omega)$ of these Celluvisc dilutions has been previously measured using a macrorheometer and time-temperature superposition by Bennett *et al.* [8]. These values, together with theoretical values of $G^*(\omega) = i\eta\omega$ in a viscous fluid can help establish the accuracy of the three different analysis methods presented in the theory section: analysis assuming a linear torque (Sec. II B); analysis that accounts for a nonlinear torque but at the expense of normalization (Sec. II C 5), and finally analysis

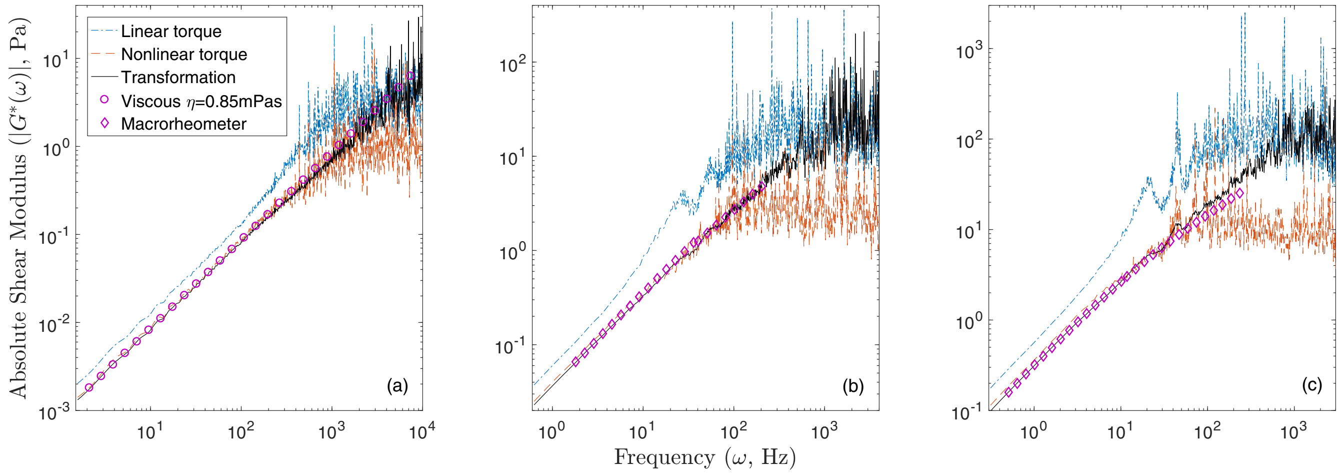

FIG. 1. A comparison between analysis methods in both viscous water and viscoelastic dilutions of Celluvisc eye drops. (a) depicts results of averaging 222 2-s flips in water, (b) 185 5-s flips in 50% Celluvisc, and (c) 90 10-s flips in 100% Celluvisc. In each graph the blue dashed line is the shear modulus calculated using the old theory, which assumes a linear restoring torque. The orange dashed lines are evaluated using the new theory accounting for the nonlinear restoring torque outlined in Sec. II C 5. The solid black line represents values obtained via the variable transformation analysis described in Sec. II C 6, which mitigates error introduced by variation in initial position. All these analysis techniques are compared to either theoretical values (circles) or macrorheological measurements [8] (diamonds).

that uses a variable transformation to account for the nonlinear torque and also allows normalization (Sec. II C 6).

The results, illustrated in Fig. 1, quite clearly demonstrate the differences in accuracy and precision of the three different analysis methods in all three fluids. The method that assumed a linear torque increased the apparent shear modulus by almost a factor of 2. This is likely because the actual torque at larger angles is much less than supposed when assuming a linear torque function. Hence, the apparent viscoelasticity is larger to compensate.

Both of the other two analysis methods, which account for the nonlinear torque function, produce values of $|G^*(\omega)|$ that have very good agreement with each other and the previous macrorheological measurements. However, the transformation method is more precise and resolves an additional decade before high frequency noise dominates the signal. Interestingly, this good agreement suggests that the flips did decay slowly relative to the fluid memory function, validating the the approximation in Eq. (32).

There are concerns about the applicability of particle tracking microrheometers inside slowly changing systems because of the long times required to obtain statistically significant averages [13]. As depicted in Fig. 2, our results demonstrate that this new theory improves the signal of each flip enough to enable precise measurements of $G^*(\omega)$ in subminute time scales.

The signal to noise ratio of only a single 5-s flip is sufficient to characterize the viscoelasticity at lower frequencies. The

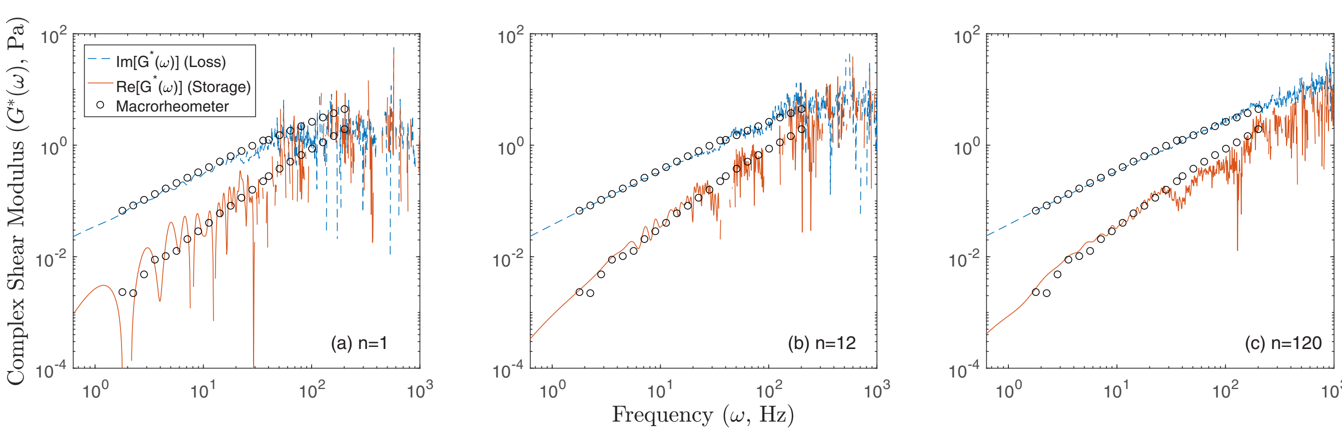

FIG. 2. The relationship between precision of $G^*(\omega)$ and the number of averaged flips in 50% Celluvisc. (a) shows the viscoelasticity obtained by analyzing a single 5s flip with the new method. (b) depicts results from 12 flips during a 1-minute measurement and (c) 120 flips during a 10-minute measurement. All three graphs show good agreement between the microrheological results (lines) and macrorheological data [8] (circles). Evidently, the precision increases with the number of averaged flips; however, because of the large amplitude of each flip, precise results can be obtained within 1 minute.

TABLE I. List of variable transformations. Ei(z) is the exponential integral function and $\gamma \approx 0.5772$ is Euler's constant.

$T(\phi)$ where $\beta > 0$	$\Psi(\phi)$	Optimal ϕ_0
$\frac{1}{\beta}\sin\beta\phi$	$\frac{2}{\beta}\tan(\frac{\beta}{2}\phi)$	$\frac{\pi}{2\beta} \leqslant \phi < \frac{\pi}{\beta}$
$\frac{1}{\beta}\tan\beta\phi$	$\frac{1}{\beta}\sin\beta\phi$	$\phi_0 = \frac{\pi}{2\beta}$
$\frac{1}{\beta}\sinh\beta\phi$	$\frac{2}{\beta}\tanh(\frac{\beta}{2}\phi)$	$\phi_0 \gg 0$
$\frac{1}{\beta}\tanh\beta\phi$	$\frac{1}{\beta}\sinh(\beta\phi)$	$\phi_0 \gg 0$
$\phi + \beta\phi^3$	$\frac{\phi}{\sqrt{1+\beta\phi^2}}$	$\phi_0 \gg 0$
$\phi - \beta\phi^3$	$\frac{\phi}{\sqrt{1-\beta\phi^2}}$	$\frac{1}{\sqrt{3\beta}} \leqslant \phi < \frac{1}{\sqrt{\beta}}$
$\frac{\phi+\beta\phi^3}{1+3\beta\phi^2}$	$\phi + \beta\phi^3$	$\phi_0 \gg 0$
$\frac{\phi-\beta\phi^3}{1-3\beta\phi^2}$	$\phi - \beta\phi^3$	$\phi_0 = \frac{1}{\sqrt{3\beta}}$
$\phi e^{-\beta\phi^2}$	$\frac{\mathrm{sign}(\phi)}{\sqrt{\beta}}\exp\{\frac{1}{2}[\mathrm{Ei}(\beta\phi^2) - \gamma]\}$	$\phi \geqslant \frac{1}{\sqrt{2\beta}}$
$\frac{\phi}{1-2\beta\phi^2}$	$\phi e^{-\beta\phi^2}$	$\phi = \frac{1}{\sqrt{2\beta}}$

presence of absolute random error does, however, affect the elastic measurements more greatly because of its larger relative size. Twelve flips greatly reduces random noise, allowing precise measurements of both viscosity and elasticity within 1 minute. Spending 10 minutes to average 120 flips does further improve the precision with diminished returns. Therefore, this new theory endows active particle tracking microrheometers with the speed necessary to explore slowly changing biological systems that were previously inaccessible.

V. CONCLUSION

Active microrheology, where a probe is impulsively driven switching between two states (two positions for translational microrheology and two orientations for rotational microrheology), can be performed with greatly improved signal to noise ratios by having larger distances or angles between the two positions or orientations. In many cases, such as where optical forces or torques are used to drive the particle, this will be outside the regime where the force or torque can be accurately approximated as a linear spring. This necessitated the development of a more general theory, not assuming linear forces.

We have presented this theory here, and shown the improvements in signal to noise that can be achieved. In addition, for some classes of problems, it is possible to further reduce error by applying a variable transformation (see Table I) which linearizes the equation of motion. This allows normalization that eliminates error introduced by low frequency drift in the particle's equilibrium position. Our measurements suggest that eliminating error can resolve viscoelasticity at an additional decade for higher frequencies. These improvements in the signal to noise ratio gives a significant reduction in the measurement time for a given error. Thus the method is more conducive to measuring viscoelasticity in slowly changing microscopic systems, such as a living cell.

ACKNOWLEDGMENTS

This research was supported under Australian Research Council's Discovery Projects funding scheme (Project No. DP140100753) as well as an Australian Government Research Training Program Scholarship.

[1] D. Weihs, T. G. Mason, and M. A. Teitell, Biophys. J. **91**, 4296 (2006).
[2] D. Robert, T.-H. Nguyen, F. Gallet, and C. Wilhelm, PLOS One **5**, e10046 (2010).
[3] P. Kollmannsberger and B. Fabry, Annu. Rev. Mater. Res. **41**, 75 (2011).
[4] S. S. Rogers, T. A. Waigh, and J. R. Lu, Biophys. J. **94**, 3313 (2008).
[5] Y.-Q. Chen, C.-Y. Kuo, M.-T. Wei, K. Wu, P.-T. Su, C.-S. Huang, and A. Chiou, J. Biomed. Opt. **19**, 011008 (2013).
[6] D. Wirtz, Annu. Rev. Biophys. **38**, 301 (2009).
[7] T. G. Mason and D. A. Weitz, Phys. Rev. Lett. **74**, 1250 (1995).
[8] J. S. Bennett, L. J. Gibson, R. M. Kelly, E. Brousse, B. Baudisch, D. Preece, T. A. Nieminen, T. Nicholson, N. R. Heckenberg, and H. Rubinsztein-Dunlop, Sci. Rep. **3**, 1759 (2013).
[9] D. Preece, R. Warren, R. M. L. Evans, G. M. Gibson, M. J. Padgett, J. M. Cooper, and M. Tassieri, J. Opt. **13**, 044022 (2011).
[10] Y. Tseng and D. Wirtz, Biophys. J. **81**, 1643 (2001).
[11] M. Tassieri, G. M. Gibson, R. M. L. Evans, A. M. Yao, R. Warren, M. J. Padgett, and J. M. Cooper, Phys. Rev. E **81**, 026308 (2010).
[12] Y. Tseng, K. M. An, and D. Wirtz, J. Biol. Chem. **277**, 18143 (2002).
[13] M. Tassieri, Soft Matter **11**, 5792 (2015).
[14] H. Lamb, *Hydrodynamics* (Cambridge University Press, Cambridge, 1895).
[15] P. Morse and H. Feshbach, *Methods of Theoretical Physics*, International Series in Pure and Applied Physics No. 1 (McGraw-Hill, New York, 1953).
[16] S. Zhang, L. J. Gibson, A. B. Stilgoe, T. A. Nieminen, and H. Rubinsztein-Dunlop (unpublished).
[17] T. A. Nieminen, N. R. Heckenberg, and H. Rubinsztein-dunlop, J. Mod. Opt. **48**, 405 (2001).